

## Comparison of microstructures in Tl-1223/Ag tapes with different chemical compositions and $J_c$ 's

D. Y. Jeong<sup>a</sup>, H. K. Kim<sup>a</sup>, H. Y. Lee<sup>a</sup>, M. K. Cha<sup>a</sup>, H. S. Ha<sup>a</sup>, S. S. Oh<sup>a</sup>,  
T. Tsuruta<sup>b</sup>, Y. Matsui<sup>b</sup>, and S. Horiuchi<sup>b</sup>

<sup>a</sup> Korea Electrotechnology Research Institute, Changwon 641-120, Korea

<sup>b</sup> National Institute for Research in Inorganic Materials, Tsukuba, Ibaraki 305-0044, Japan

The microstructures of a  $Tl_{0.8}Pb_{0.2}Bi_{0.2}Sr_{1.6}Ba_{0.4}Ca_2Cu_3O_{9+\delta}/Ag$  tape (tape I) with  $J_c$  of 17,600 A/cm<sup>2</sup> at 77 K and 0 T and three  $Tl_{0.8}Pb_{0.2}Bi_{0.2}Sr_{1.8}Ba_{0.2}Ca_{2.2}Cu_3O_{9+\delta}/Ag$  tapes with  $J_c$ 's of 9,300 (tape II), 16,700 (tape III) and 25,200 A/cm<sup>2</sup> (tape IV) prepared using the powder-in-tube method and an in-situ reaction method, were investigated using scanning electron microscopy and high-resolution transmission electron microscopy, and compared each other. In the tape preparation, an intermediate rolling process was incorporated during final heat-treatment for the last tape, but not for the rest of the tapes. The microstructural analysis revealed clear differences in grain-texturing, crystallographic defects and impurity phases, depending on the chemical composition of the tape. Tendency of directional grain-alignment increased in an order of tapes I, II, III and IV. In tape IV, Tl-1223 grains are textured, at least in local regions. In crystallographic defects, while stacking faults were prevalent in the former composition, dislocations and voids were frequently observed in the latter. Also impurity phases were appeared to be more abundant in the former than in the latter. The relationship between  $J_c$  and the microstructure in the tapes was attempted to explain in a term of grain-linking.

### 1. Introduction

It has been known that Tl-1223 superconductor has an irreversibility line located at a relatively high position in H-T space, which is due to the relatively short distance between Cu-O layers in the crystal lattice, compared to those of other high  $T_c$  superconductors [1]. Therefore, it has been expected that Tl-1223 wires with large current-carrying capacities at relatively high fields and temperatures will be able to developed and realize 40 K technology instead of 20 K in the case of Bi-based superconducting wires.

Different from remarkable advances [2,3] in

aspects of  $J_c$  and preparation cost in Tl-1223 film-type tapes prepared by so-called open methods, the progress in preparation of Tl-1223 tapes with high  $J_c$ 's by using the powder-in-tube (PIT) method has been slowed down. Tl-1223 tapes prepared by the PIT method have revealed poor connectivity and little directional alignment of Tl-1223 grains in the superconducting cores of the tapes [1,4,5], and thus resulted in relatively low  $J_c$ 's compared to that of Bi-based high- $T_c$  superconducting tapes. Up to now, various chemical compositions and preparation methods have been tried [4-19] in order to prepare the tapes with high  $J_c$ 's. It has been found that the grain-connectivity and

degree of directional grain-alignment, and thus  $J_c$  values primarily depended on the nominal compositions used for the tape cores - especially the ratio of Sr to Ba in the compositions [6,13,16,19]. The tapes of compositions with Sr:Ba=1.6:0.4 such as  $Tl_{0.92}Bi_{0.22}Sr_{1.6}Ba_{0.4}Ca_2Cu_3O_z$  [4,5] and  $Tl_{0.8}Pb_{0.2}Bi_{0.2}Sr_{1.6}Ba_{0.4}Ca_2Cu_3O_z$  [16], have revealed ill-defined Tl-1223 grains and little directional grain-alignment. A relatively high  $J_c$  of  $1.8 \times 10^4$  A/cm<sup>2</sup> at 77 K and 0 T was obtained in a just-rolled tape of  $Tl_{0.8}Pb_{0.2}Bi_{0.2}Sr_{1.6}Ba_{0.4}Ca_2Cu_3O_z$  due to a little enhanced grain-connectivity [16]. On the other hand, the tapes of composition with Sr:Ba=1.8:0.2 have revealed plate-like Tl-1223 grains and a clear tendency of directional grain-alignment [7,19]. Thus a further high  $J_c$  of  $2.5 \times 10^4$  A/cm<sup>2</sup> at 77 K and 0 T was obtained in just-rolled tapes of  $Tl_{0.8}Pb_{0.2}Bi_{0.2}Sr_{1.8}Ba_{0.2}Ca_{2.2}Cu_3O_z$  nominal composition [19]. The high  $J_c$  value was attributed to enhancement in grain-connectivity by intermediate rolling, which is assisted by the retarded decomposition of Tl-1223 phase in the composition.

In the present study, the microstructures in tapes of  $Tl_{0.8}Pb_{0.2}Bi_{0.2}Sr_{1.6}Ba_{0.4}Ca_2Cu_3O_{9+\delta}$  and  $Tl_{0.8}Pb_{0.2}Bi_{0.2}Sr_{1.8}Ba_{0.2}Ca_{2.2}Cu_3O_{9+\delta}$  compositions with different preparation history and thus different  $J_c$  values were investigated using scanning electron microscopy and high-resolution transmission electron microscopy, and compared each other in viewpoints of density, grain size, grain-texture, linking between grains, defects and voids in grains and impurity phases.

## 2. Experimental

Tl-1223/Ag tapes of  $Tl_{0.8}Pb_{0.2}Bi_{0.2}Sr_{1.6}Ba_{0.4}Ca_2-Cu_3O_{9+\delta}$  and  $Tl_{0.8}Pb_{0.2}Bi_{0.2}Sr_{1.8}Ba_{0.2}Ca_{2.2}Cu_3O_z$  nominal compositions were prepared using the power-in-tube method incorporating an in-situ reaction method as follows :

Sr-Ba-Ca-Cu-O prepowder and  $Tl_2O_3$ , PbO

and  $Bi_2O_3$  powders were mixed in stoichiometric ratios according to  $Tl_{0.8}Pb_{0.2}Bi_{0.2}-Sr_{1.6}Ba_{0.4}Ca_2Cu_3O_{9+\delta}$  and  $Tl_{0.8}Pb_{0.2}Bi_{0.2}Sr_{1.8}Ba_{0.2}-Ca_{2.2}Cu_3O_z$  compositions, and filled into Ag-tubes. 0.1 mole of excessive  $Tl_2O_3$  in the compositions was added to compensate Tl loss during the tape preparation process, which was estimated by an ion-coupled plasma analysis. The tubes for the former and the latter compositions were drawn to wires ~1.0 and ~1.2 mm in diameter, respectively, rolled to tapes 0.5 mm in thickness, and cut to tapes 1 m long. Then the tapes for the former and the latter compositions were heat-treated in 840°C for 25 and 20 min, respectively. The tapes were rolled to tapes 0.10~0.13 mm thick and cut to pieces ~5 cm long. Then a tape for the former composition was heat-treated at 835°C for 7 h. (Tape I) The tapes of the latter were heat-treated at 840°C for 4, 7 (tape III) and 15 h (tape II), respectively. The tape heat-treated for 4 h was rolled to 0.09 mm in thickness, and heat-treated at 840°C for 4h. (Tape IV). It should be mentioned that for rolling the tapes, a twin roller of 100 mm in diameter were used for the former composition, and that of 150 mm for the latter. The further details on preparation of the tapes were shown in elsewhere [16,19].

$J_c$ 's of the tapes were evaluated using dc four-probe electrical measurements after immersing them into liquid nitrogen. The phases present in the tape cores were investigated using a Philips PW 1710 x-ray diffractometer (XRD) using a Cu  $K_\alpha$  target. The XRD measurements were performed after peeling off the Ag-sheath on one side using a blade. The microstructure of the tapes was examined using a Hitachi S-2700 scanning electron microscope (SEM) with an accelerating voltage of 20 kV and a Hitachi H-1500 high-voltage transmission electron microscope (TEM) with an accelerating voltage of 800 kV. The scanning electron microscopy was examined on the core surfaces of

the tapes after peeling off the Ag-sheath on one side using a blade. The transmission electron micrography was examined on the longitudinal cross-sections of the tapes. The details on the specimen preparation for the cross-sectional view were shown in elsewhere [20].

### 3. Results

#### 3.1. Transport properties of specimens

Table 1 shows  $J_c$ 's and  $I_c$ 's at 77 K and 0 T, thicknesses and preparation histories of the tapes investigated in the present study. Tape I was prepared using a  $Tl_{0.8}Pb_{0.2}Bi_{0.2}Sr_{1.6}Ba_{0.4}Ca_2Cu_3O_{9+\delta}$  nominal composition. Tapes II, III and IV were prepared using a  $Tl_{0.8}Pb_{0.2}Bi_{0.2}Sr_{1.8}Ba_{0.2}Ca_{2.2}Cu_3O_{9+\delta}$ .  $J_c$ 's at 77 K and 0 T of tapes I, II, III and IV are 17,600, 9,200, 16,700 and 25,200 A/cm<sup>2</sup>, respectively. It should be noted that tape III is much thicker than others, probably due to the volume expansion resulting from prominent directional-growth of randomly aligned Tl-1223 grains during the relatively long heat-treatment. It is also worthwhile to note that tape IV was prepared by incorporating an intermediated rolling processing during the final heat-treatment.

Table 1.  $J_c$ 's and  $I_c$ 's at 77 K and 0 T, thicknesses (t) and preparation histories of the tapes investigated in the present study. Tape I was prepared using a  $Tl_{0.8}Pb_{0.2}Bi_{0.2}Sr_{1.6}Ba_{0.4}Ca_2Cu_3O_{9+\delta}$  nominal composition. Tapes II, III and IV were prepared using a  $Tl_{0.8}Pb_{0.2}Bi_{0.2}Sr_{1.8}Ba_{0.2}Ca_{2.2}Cu_3O_{9+\delta}$ .

Tape no.	$J_c$ (A/cm <sup>2</sup> )	$I_c$ (A)	t (mm)	Preparation history
I	17,600	11.04	0.101	840°C/25min+R+835°C/7h
II	9,300	11.61	0.151	840°C/20min+R+840°C/15h
III	16,700	16.92	0.112	840°C/20min+R+840°C/7h
IV	25,200	21.23	0.090	840°C/20min+R+840°C/4h +R+840°C/4h

Fig. 1 shows the field dependence of  $I_c$  at 77 K of tapes I, II, III and IV. In the inset, the

$I_c$  values are normalized to  $I_c(H)/I_c(0)$ . The Both tapes reveal almost same strong dependence on magnetic field. However, larger portion of current paths survived in high fields in tape IV than in tape I. Fitting the curve at high fields to low fields indicated that the strong link fractions in tapes I, II, III and IV are 2.0, 1.6, 2.3 and 4.1%.

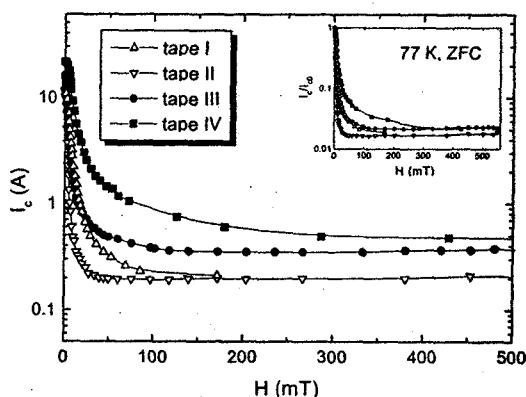


Fig. 1. The field dependence of  $I_c$  of tapes I, II, III and IV measured at 77 K. In the inset,  $I_c(H)$  is normalized by  $I_c(0)$ .

#### 3.2. X-ray diffraction analysis

Fig. 2(a), (b), (c) and (d) show XRD patterns taken in tapes I, II, III and IV, respectively. It shows that all the tapes are consisted of a major 1223 phase, minor 1212, and very small amounts of secondary phases such as  $BaPbO_3$ ,  $(Sr,Ca)_{14}Cu_{24}O_x$ ,  $(Sr,Ca)_2CuO_3$ ,  $CuO$  etc. It is noted that the intensities of (00l) peaks are most prominent in tape IV than any other tapes, indicating that the intermediate rolling during final heat-treatment is effective in aligning Tl-1223 grains in a preferred orientation.

The weight percentages of phases contained in the tapes, which were estimated from Fig. 1 by using a "simplicity" method [21], are listed in Table 2. It is noted in Table 2 that tape I contains the largest amount of impurity phases among the tapes - especially  $BaPbO_3$ , and

detectable amount of unreacted starting oxides. Table 2 also indicates that the Tl-1223 content increases in an order of tapes I, II, III and IV.

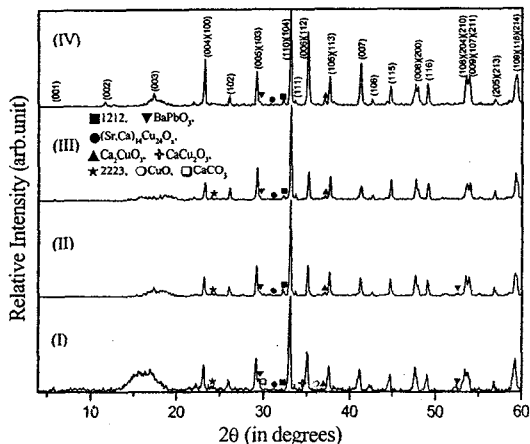


Fig. 2. XRD patterns taken in tapes (a) I, (b) II, (c) III and (d) IV.

Table. 2. Weight percentages of phases contained in tapes used for the present study. The percentages were calculated using the "simplicity" method [21]. 14:24, 2:1 and 1:2 stand for  $(\text{Sr,Ca})_{14}\text{Cu}_{24}\text{O}_x$ ,  $\text{Ca}_2\text{CuO}_3$ , and  $\text{CaCu}_2\text{O}_3$ , respectively.

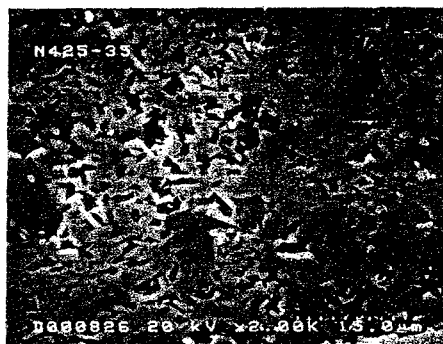
Tape no.	Weight percentages of phases contained in each tape core								
	1223	1212	2223	BaPbO <sub>3</sub>	14:24	2:1	1:2	CuO	CaCO <sub>3</sub>
I	72.42	2.48	4.12	9.39	0.84	1.65	3.40	2.78	2.88
II	84.45	6.35	2.45	3.72	1.93	1.09	0	0	0
III	87.95	3.57	3.50	3.07	1.02	0.89	0	0	0
IV	88.74	4.79	0	3.53	1.72	1.21	0	0	0

### 3.3. Scanning electron microscopy

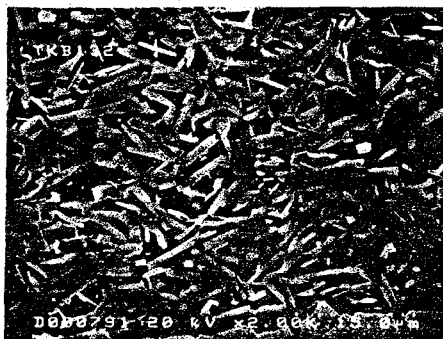
Fig. 3(a,b,c,d) shows SEM secondary electron images taken in tapes I, II, III and IV, respectively.

In tape I, it was identified from an EDS analysis that gray grains with arbitrary shapes are Tl-1223, a little more darker ones  $(\text{Ca,Sr})\text{Cu}_2\text{O}_3$  impurities, and much darker ones  $(\text{Ca,Sr})_2\text{CuO}_3$ . The Tl-1223 grains are relatively ill-defined compared to those in other tapes,

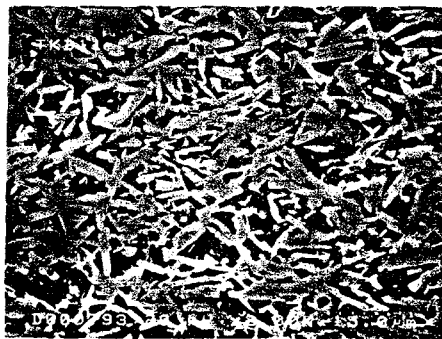
randomly aligned, and sometimes mixed with impurities. The average size of the grains is estimated to be about 5  $\mu\text{m}$ . The enlarged picture of Fig. 3(a), which is not shown in the present paper, indicates that the grains seem to have a substructure, which indicates that they consisted of stacks of inter-grown platelets. The Tl-1223 grains seemed to be well connected through ab-planes, besides through c-axis grain boundaries.



(a)



(b)



(c)



(d)

Fig. 3. SEM images taken in tapes (a) I, (b) II, (c) III and (d) IV.

In tapes II, III and IV, gray platelets are TI-1223, and darker gray ones  $(Ca,Sr)_2CuO_3$ . The TI-1223 platelets are well-defined, and tend to align along the rolling direction. The tendency appears to be relatively weak in tape II and III, but very strong in tape IV. As a matter of fact, it can be said that TI-1223 grains in tape IV are textured, at least in local regions, as can be clearly identified in the lower middle region of Fig. 3(d). The highly textured microstructure in tape IV compared to those in tapes II and III, indicates that the intermediate rolling is very effective in grain-texturing. This fact is consistent with the conclusion of XRD analysis of Fig. 2. By the way, the upper region of Fig. 3(d) indicates that the grain-texturing in orders of macroscopic range is hindered by pores and impurities. The TI-1223 grains seem to be mostly connected through c-axis grain boundaries. Connection through ab-planes are rarely observed. The average grain sizes in tapes II and III are estimated to be about 8  $\mu m$ . In tape IV, the size is a little reduced to less than 6  $\mu m$ , probably due to the intermediate rolling during final heat-treatment. In  $Tl_{0.8}Pb_{0.2}Bi_{0.2}Sr_{1.8}Ba_{0.2}Ca_{2.2}Cu_3O_x$  tapes, as the intermediate rolling was incorporated, the pore density and size, in addition to the grain size, was much reduced, and thus the core density

much increased.

In Fig. 3, the core density seems to increase in an order of tapes II, III, IV and I. The grain morphology is different depending on the chemical composition used for the tape. The grains in tape I are chunky and those in tapes II, III, and IV needle-like, even though it is believed the sub-grains in all the tapes, which consists the grains, are basically same as platelets. The difference in the grain morphology has been attributed to the difference in chemical composition used for the tape preparation, especially the difference in the ratio of Sr to Ba [22]. By the way, it was strange that even though the content of  $(Ca,Sr)_2CuO_3$  in the tape was estimated to be  $\sim 1$  wt.% from analysis of XRD patterns shown in Fig. 2, the majority of impurities contained in the tapes was identified to be  $(Ca,Sr)_2CuO_3$  by EDS analysis. Also,  $BaPbO_3$  phase was rarely observed in SEM analysis.

#### 3.4. Transmission electron microscopy

Fig. 4 show TEM images taken in tapes I, II, III and IV. In the figures, poorly transparent substances with rod-like shape are TI-1223 platelets and a little more transparent ones impurity phases. Much more transparent ones in tape I are thought to be glue used for sticking the tapes together during the TEM specimen preparation. Fig. 4 shows that there are clear differences in shape and alignment of TI-1223 grains, connection among TI-1223 grains and size and amount of impurity phases among the present tapes.

In Fig. 4(a), TI-1223 grains are ill-defined, so that little information on grain-alignment is available. It can be recognized, however, that TI-1223 grains are bonded with many impurities, the linking among the grains may be significantly deteriorated. In Fig. 4(b,c,d), on the other hand, the grains are well-defined as platelets, so that clear information on grain-alignment is available. In tapes II, III and IV,

the grains tend to be aligned in preferred orientations. The tendency of grain-alignment in preferred orientation is relatively much weak in tapes II and III, but that very strong in tape IV. Actually, it can be said that the grains in tape IV are textured, at least in the lower center region of Fig. 3(d).



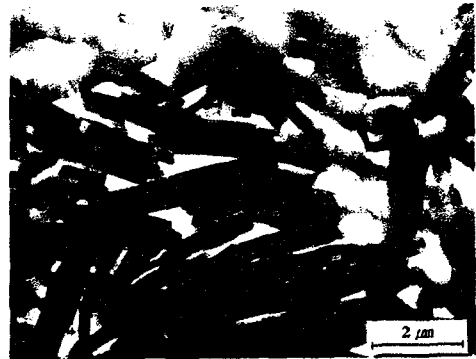
(a)



(b)



(c)



(d)

Fig. 4. TEM images taken in tapes (a) I, (b) II, (c) III and (d) IV.

In Fig. 4(b,c,d), TI-1223 grains seem to be connected to each other by sharing small common areas on their lateral edges and ends. A clear picture of such a connection through the lateral edges and ends is shown in Fig. 5, which was taken in tape II. In Fig. 4(b,c), the linking among TI-1223 grains is poor. In other words, the contact area and the frequency of the connection are small. Careful comparison of tape II and III reveals that they are smaller in tape II than in tape III. However, they are much enhanced in tape IV. Therefore, it can be concluded that the linking among the grains becomes strong in an order of tapes II, III and IV.

Fig. 6 shows a TEM image taken in tape IV, in which a TI-1223 platelet is composed of many sub-grains whose boundaries are marked by asteroids. Along the boundaries, many small holes occur. The boundaries seems to be of several types. It is worthwhile to note in Fig. 6 that TI-1223 platelets are hardly connected in the c-direction. Fig. 7 shows a TEM image taken in a portion different from that for Fig. 6 in tape IV, revealing kinds of the sub-grain boundary present in the tape. The boundary located in bottom part of Fig. 7 is believed to be a small-angle mixed-type of tilt and twist boundaries with an tilt angle of  $2^\circ$ . The

boundary is slightly bent. The upper one in Fig. 7 is a high-angle pure-tilt boundary with an angle of  $12^\circ$ . The former type was frequently observed in  $Tl_{0.93}Bi_{0.22}Sr_{1.6}Ba_{0.4}Ca_2Cu_3-O_z$  tapes [20].



Fig. 5. A SEM image taken in tape II, showing that TI-1223 grains are connected to each other by sharing small common areas on their lateral edges and ends.

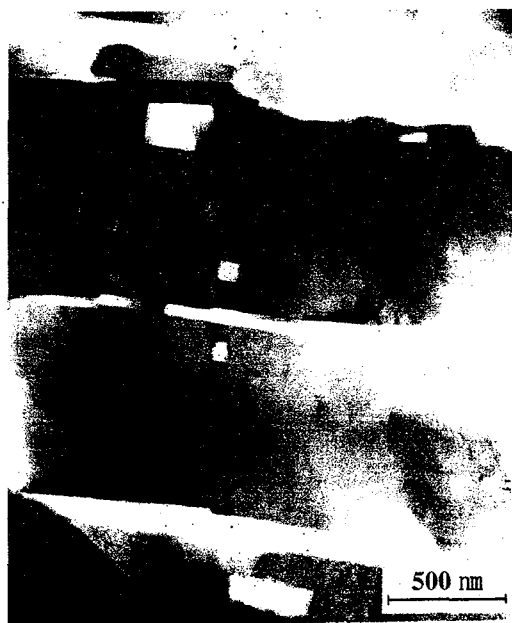


Fig. 6. A TEM image taken in tape IV, showing that a TI-1223 platelet is composed of many sub-grains.

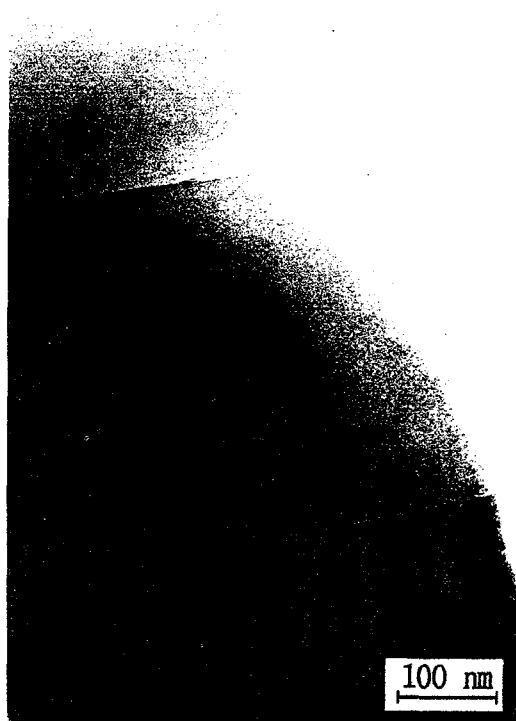


Fig. 7. A TEM image taken in tape IV, showing types of sub-boundaries.

Also there were clear differences in kinds of crystallographic defects present in the tapes, probably depending on the chemical composition and mechanical working used, as will be discussed later. The line networks with a little darker contrast inside TI-1223 grains in Fig. 4(b,c,d) and Fig. 5 are believed to be dislocations. The dislocations were dominantly observed in tapes II, III and IV, but are relatively rare in tape I. In tape I, instead, stacking faults were prevalently observed with strain fields which become strong as approaching the center of the grains. Fig. 8 shows stacking faults occurred in a TI-1223 grain in tape I, which are marked by asteroids. Also small holes, which were found for the first time in our previous work [20], were frequently observed in tapes II, III and IV but

rarely observed in tape I, as can be recognized from Fig. 4 and Fig. 6.

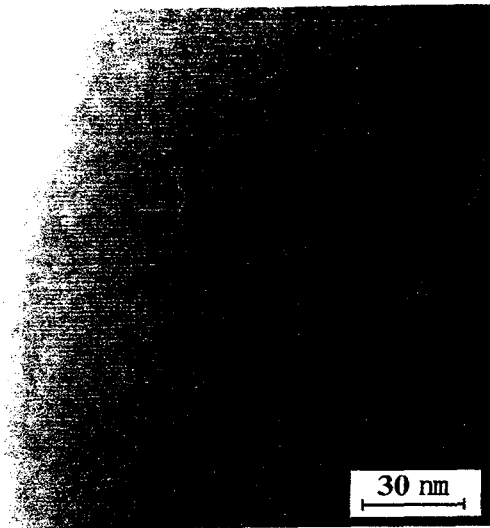


Fig. 8. A TEM image taken in tape I, showing the occurrence of stacking faults (dark, narrow stripes) at the grain edge. The darker, wide bands are strain fields.

Finally, TEM observation on many portions of the specimens indicated that the contents of Tl-1223 phase increased in an order of tapes I, II, III and IV. Also the amount and the size of impurity phases and pores decreased in an order of tapes I, II, III and IV. These observations were consistent with the XRD result shown in Table 2 and the SEM observation of Fig. 3. The sizes of impurities in tape IV appeared to be much smaller than those of others. The much smaller size is believed to result from the intermediate rolling incorporated during the final heat-treatment of the tape.

The results of TEM observation on tapes I, II, III and IV were summarized in Table 3.

#### 4. Discussion

The primary concern of the present study lies in which factors in microstructure critically

affect the  $J_c$  value of Tl-1223 tape. Up to now, the  $J_c$  value in Tl-1223 tapes of (Tl,Pb or Tl-Bi)-(Sr,Ba)-Ca-Cu-O has mainly depended on core density, which has directly reflected the grain-connectivity. In the present study, however, the core density seems not to be a direct indication of  $J_c$  value any more, because the order in magnitude of core density does not coincide with that in  $J_c$  value. Furthermore, while the above two composition systems and tape I reveal no significant directional grain-alignment, tape II, III, and IV reveals clear tendency of directional grain-alignment. The grains in some regions of tape IV are even textured. So it may be expected that the concept of directional grain-alignment explains the  $J_c$  difference between tapes I and IV. However, a similar field-dependence of  $J_c$ 's in both tapes shown in Fig. 1 ruins such an expectation. Therefore, it is believed that some other factors or concepts are required to explain the  $J_c$  difference.

The difference in microstructure between tapes I and IV is estimated to be the grain shape, amount of impurities, degree of directional grain-alignment and linking among the grains. By the way, the key one in above terms is thought to be grain-linking, because all the above factors including the core density are supplementary ones for determining a state of grain-linking which directly determines the current-carrying capacity. For example, the grain shape is related to the  $J_c$  value not directly, but indirectly through geometrical arrangement of grains, because it guides geometrical arrangement of grains and the geometrical arrangement of grains itself is a state of close packing and a measure of degree of directional grain-alignment, which is a measure of grain-linking.

The links among grains is thought to be determined by three characteristic parameters, i.e., frequency of grain-connection, contact area, and junctional characteristics of the links. The



frequency and the contact area are governed by grain shape, core density, impurity and degree of directional grain-alignment. The junctional characteristics are governed by intrinsic coupling strength and type of grain boundary. In this context, comparison of the links in tapes I and IV based on the results of Figs. 1 to 4 is as follows: The frequency and the contact area are expected to be larger in tape I than tape IV, due to the relatively large core density in tape I. However, the impurities in tape I are mixed and bonded to TI-1223 grains, as shown in Figs. 3 and 4, and expected to hinder the contact and reduce the contact area. On the other hand, as the grains in tape IV are directionally aligned, the frequency and the contact area will be larger than that expected from its a little lower density. Also the directional grain-alignment will increase the density of small-angle grain boundaries such as small-angle c-axis tilt boundary and edge-on c-axis tilt boundary, which are claimed to be responsible for strong links in the regime of "railway switch" model [23,24]. So the density of small-angle boundaries is expected to be larger in tape IV than in tape I. There are no firm experimental evidences to support the differences in physical properties resulting from the difference in small-angle boundary density between both tapes. Loose evidences up to now are that the inter-granular decoupling temperature under 15 Oe of ac field in ac susceptibility measurement was about 90 K and around 100 K for tapes I and IV, respectively [25], and the fractions of strong-link in tapes I and IV are 2.1 and 4.1%, respectively, which are calculated by extending the curve in high fields to low fields in Fig. 1. For firm evidences, the ac susceptibility should be measured under relatively high fields greater than 100 Oe, and the field dependence of  $J_c$  near 40 K.

Even though the above evidences are not

enough to explain the difference in grain-linking between both tapes, the differences in physical properties are much smaller than that expected from viewpoint of the difference in the frequency and area of grain-contact, and the small-angle boundary density. Therefore, another factor is required to compensate such small differences. What left in the above factors in consideration is intrinsic coupling strength of grain-boundary junction. It is thought that the intrinsic coupling strength is weaker in tape IV than in tapes I. Ac susceptibility measurement indicated that inter-granular junctions in both tapes are basically SIS type, but that in tape I has a little more SNS characteristic. Clear elucidation of the above inference is left for further studies.

In the present study, defects present in the tapes appeared to be different depending on kind of the tape. While stacking faults were prevalently observed in tape I with strain fields, dislocations were dominantly observed in tapes II, III and IV. Also holes were frequently observed in the latter tapes but rarely observed in the former. The possible sources responsible for the occurrence of such different defects are thought to be different nominal compositions used for the tape cores and different magnitude of stress exerted during rolling due to different diameters of twin roller used, because these two are only the difference in the preparation parameters used for the tape preparation. As a larger twin roller was used for the latter tapes than for the former, the density of dislocations generated by rolling is likely to be higher in the latter than in the former. It is expected, however, that the dislocations in both tapes are removed during heat-treatment process following the rolling, and their density should not be much different in both kinds of tapes. However, what really happened was different depending on the kind of tapes. During the heat-treatment, the dislocations in tape I were

relatively easily relieved and left stacking faults with strain fields, as indicated by Fig. 9. On the other hand, the majority of the dislocations in tapes II, III and IV still remained after the heat-treatment, as indicated by Fig. 4(b,c,d) and Fig. 5. That means that the majority of the dislocations were locked by certain pinning centers. Fig. 5 shows that the sub-grain boundaries are one of the possible pinning centers, because the dislocation line are ended at sub-boundaries rather than free-edges of grain.

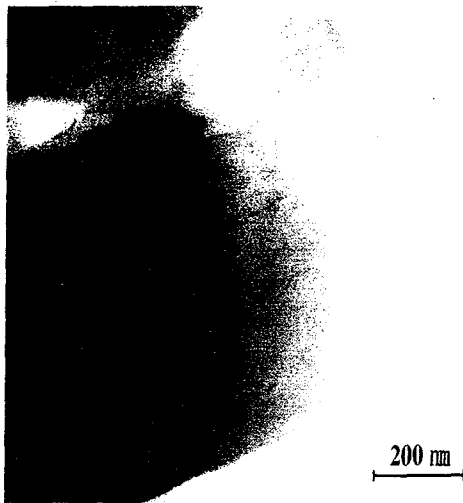


Fig. 9. A TEM image taken in tape I, showing the relation between strain fields and stacking faults. Stacking faults occur at the edge of Tl-1223 grain where strain fields are developed inside.

### Acknowledgement

The present authors express their gratitude to Korean Ministry of Science and Technology and Japanese Science and Technology Agency for their financial support.

### References

[1] M. Jergel, A. Conde Gallardo, C. Falcony Guajardo and V. Strbik,

Supercond. Sci. Technol. 9, 427 (1996).  
 [2] National Renewable Energy Lab. report, Superconductor Week, Vol. 12, No. 9, 1 (1998).  
 [3] Z. F. Ren, W. Li, D. Z. Wang, J. Y. Lao, J. H. Wang, M. Paranthaman, D. T. Verebelyi, D. K. Christen, D. F. Lee, A. Goyal and D. M. Kroeger, Physica C 313, 241 (1999).  
 [4] Z. F. Ren, J. H. Wang, D. J. Miller and K. C. Goretta, Physica C 229, 137 (1994).  
 [5] D. J. Miller, J. G. Hu, Z. Ren and J. H. Wang, J. Electro. Mater. 23, 1151 (1994).  
 [6] Z. F. Ren and J. H. Wang, Physica C 216, 199 (1993).  
 [7] K. A. Richardson, S. Wu, D. Bracanovic, P. A. J. de Groot, M. K. Al-Mosawi, D. M. Osborne and M. T. Weller, Supercond. Sci. Technol. 8, 238 (1995).  
 [8] G. E. Gladyshevskii, A. Perin, B. Hensel, R. Flukiger, R. Abraham, K. Lebbou, M. Th. Cohen-Adad and J. -L. Jordan, Physica C 255, 113 (1995).  
 [9] Z. F. Ren, C. A. Wang, J. H. Wang, D. H. Miller and K. C. Goretta, Physica C 247, 163 (1995).  
 [10] V. Selvamanickam, T. Finkle, K. Pfaffenbach, P. Haldar, E. J. Peterson, K. V. Salazaar, E. P. Roth, and J. E. Tkaczyk, Physica C 260, 313 (1996).  
 [11] M. R. Hagen, D. S. Kupperman, K. C. Goretta and M. T. Lanagan, Supercond. Sci. Technol. 9, 898 (1996).  
 [12] M. T. Lanagan, J. Hu, M. Foley, P. Kostic, M. R. Hagen, D. J. Miller and K. C. Goretta, Physica C 256, 387 (1996).  
 [13] V. Selvamanickam, K. Pfaffenbach, D. Kirchoff, M. Gardner, D. W. Hazelton and P. Haldar, IEEE Trans. Appl. Supercond. 7, 1953 (1997).  
 [14] J. C. Moore, D. M. C. Hyland, C. J. Salter, C. J. Eastell, S. Fox, C. R. M. Grovenor and M. J. Goringe, Physica C 276, 202 (1997).  
 [15] D. Y. Jeong and M. H. Sohn, J. Kor. Phys. Soc. 31, 60 (1997).  
 [16] D. Y. Jeong and M. H. Sohn, Physica C 297, 192 (1998).  
 [17] T. Riepl, S. Zachmayer, R. Low, C.

- Pauli, C. Reimann and K. F. Renk, *J. Supercond.* **11**, 67 (1998).
- [18] C. M. R. Grovenor, J. C. Moore, C. J. Eastell, M. J. Naylor, S. Fox, V. Boffa, R. Bruzzese and M. J. Goringe, *J. Supercond.* **11**, 103 (1998).
- [19] D. Y. Jeong, H. K. Kim and Y. C. Kim, *Physica C* **314**, 139 (1999).
- [20] D. Y. Jeong, M. H. Sohn, H. S. Kim, L. L. He, M. Cantoni and S. Horiuchi *Physica C* **269**, 279 (1996).
- [21] W. W. Schmahl, M. Lehmann, S. R ath, M. Gerards and R. Riddle, *Supercond. Sci. Technol.* **11**, 1269 (1998).
- [22] S. Heede, M. Ullrich, H. C. Freyhardt, R. E. Gladyshevskii, E. Bellingeri and R. Flukiger, *J. Supercond.*, **11**, 97 (1998).
- [23] B. Hansel, J. -C. Grivel, A. Jeremie, A. Perin, A. Pollini and R. Flukiger, *Physica C* **205**, 329 (1993).
- [24] B. Hansel, G. Grasso and R. Flukiger, *J. Electro. Mater.* **24**, 1877 (1995).
- [25] D. Y. Jeong, H. K. Kim, M. H. Sohn, B. J. Kim, Y. C. Kim, H. S. Ha and S. S. Oh, "High  $J_c$ 's in Just-rolled Tl-1223/Ag Tape s" High Temperature Superconductivity Vol. VIII (Proc. of the 8th Korean Conf. on Materials and Applications of Superconductivity, Aug. 19-21, 1998, Yongpyeong, Korea) 165-168.